Payload-Directed Control of Geophysical Magnetic Surveys

Ritchie Lee[1], Yoo-Hsiu Yeh[2]
Carnegie Mellon University Silicon Valley Campus, Moffett Field, CA, 94035

Corey Ippolito[3]
NASA Ames Research Center, Moffett Field, CA, 94035

John Spritzer, Geoffrey Phelps
United State Geological Survey, Menlo Park, CA, 94025

Using non-navigational (e.g. imagers, scientific) sensor information in control loops is a difficult problem to which no general solution exists. Whether the task can be successfully achieved in a particular case depends highly on problem specifics, such as application domain and sensors of interest. In this study, we investigate the feasibility of using magnetometer data for control feedback in the context of geophysical magnetic surveys. An experimental system was created and deployed to (a) assess sensor integration with autonomous vehicles, (b) investigate how magnetometer data can be used for feedback control, and (c) evaluate the feasibility of using such a system for geophysical magnetic surveys. Finally, we report the results of our experiments and show that payload-directed control of geophysical magnetic surveys is indeed feasible.

I. Introduction

DUE to the difficulty in extracting meaningful navigation information from non-navigational sensors, mission payload sensors are typically segregated from navigation systems to collect their data independently. Ironically, payload sensor data is usually the primary driver for the mission (e.g. when tracking or mapping a phenomenon using application-specific sensors). This lack of communication between the payload sensor and the navigation system forces one of two vehicle operational modes:

1) The vehicle follows a pre-determined trajectory path, such as fixed waypoints or a survey grid.
2) Human operators are responsible for determining the trajectory path during the mission.

Uncertainties in the a priori knowledge of the mission environment and the inability of human operators to adequately process payload sensor measurements in real-time limit the value of sensor return while operating in these modes. To maximize sensor return, it is not only necessary to enable communication between the various onboard systems, but also to establish a framework to encourage their cooperation towards mission objectives. Through intelligent cooperation between the autopilot and onboard mission payload sensors, next generation autonomous vehicles can take advantage of greater data availability to better achieve their mission objectives. Whether the mission objectives are mapping, tracking, or surveillance, the ability to close the loop around mission payload sensors using intelligent autonomous algorithms provides increased efficiency and performance as well as exciting next-generation capabilities to vehicle platforms.

Using non-navigational (e.g. imagers, scientific) sensor information in control loops is a difficult problem to which no general solution exists. Whether the task can be successfully achieved in a particular case depends highly on problem specifics, such as application domain and sensors of interest. In this study, we investigate the feasibility of using magnetometer data for control feedback in the context of geophysical magnetic surveys.

The idea of payload-directed control is not a completely novel one in the realm of geophysical surveys. When performing geophysical surveys, there typically exists a tradeoff between performing high-resolution surveys, which provide more information, and low-resolution surveys, which are faster to perform. Consider a geophysical survey whose purpose is the characterization of a geologic phenomenon. In the case where the location of the phenomenon

[1] Research Scientist, Carnegie Mellon Innovations Lab, Carnegie Mellon University Silicon Valley, AIAA Member.
[2] Project Engineer, Carnegie Mellon Innovations Lab, Carnegie Mellon University Silicon Valley, AIAA Member.
[3] Research Scientist, Intelligent Systems Division, NASA Ames Research Center, AIAA Member.

is already known, one's best course of action would naturally be to perform an exhaustive high-resolution survey over that particular area. However, if the survey area is large and the exact locations of interest are not known a priori, then an exhaustive survey over the entire area would be highly inefficient. In such a situation, a common technique is to first perform a low-resolution survey over the entire area, have a human expert assess the data at a high-level for potential target areas, and then perform high-resolution surveys over those identified areas. In this fashion, human judgment tries to focus surveying efforts towards areas of higher scientific value. Autonomous payload-directed control follows this similar approach, but extends it much further using autonomous system technologies.

There are several key differences between the human-operated survey and the payload-directed autonomous survey. First, models and sensor processing algorithms are used for sensor data interpretation. Secondly, the constraint of a pre-determined vehicle trajectory is removed, and the vehicle path is chosen in real-time using multi-objective optimization techniques that maximize mission-level objectives. Finally, since the feedback loop does not involve humans, the cycle may be executed at much higher frequencies. The main idea is to enable the autonomous system to distinguish scientifically interesting regions from uninteresting ones, allowing real-time adaptation of the trajectory. The result is potential time-savings, more efficient coverage, and improved scientific return on the survey data.

We proceed to investigate the feasibility of applying payload-directed control technologies towards the performance of geophysical magnetic surveys by focusing on the following key questions:

a) Can magnetometer systems be used with autonomous platforms?
b) Can magnetometer data be used in feedback control?
c) Can such a system be used to correctly identify and map magnetic features?

We begin in Section II by giving background information on Payload-Directed Flight (PDF) and describing the overall mission concept for payload-directed control for geophysical surveys. Section 0 details the experimental setup targeted at answering the above questions. Finally, the results of this study are shown and discussed in Section IV.

II. Background

A. Payload-Directed Flight

The main concept of Payload-Directed Flight (PDF) is to enable control loop closure around payload sensors, such as imagers and other scientific instruments. Research into Payload-Directed Flight examines payload-centric autopilot modes, architectures, and algorithms that provide layers of intelligent guidance, navigation and control for flight vehicles. These layers achieve mission goals related to the payload sensors, taking into account various constraints such as the performance limitations of the aircraft, target tracking and estimation, obstacle avoidance, and constraint satisfaction.

The central problem addressed by PDF is the control of a known and controllable vehicle interacting with an external system to satisfy mission objectives and constraints on the combined system. In particular, the interaction is based on payload and sensor data feedback that gives a partial observation and understanding of the external system. This research focuses on (a) trajectory generation and flight control under varying constraints in a highly dynamic environment, (b) autonomous feature detection and estimation, and (c) modeless autopilot design concepts for multi-objective system control. Application of this research is targeted towards increasing capabilities, performance, and efficiency in the execution of missions that require payload-directed and target-directed maneuvering. The applications of this technology include hurricane monitoring, formation flying, weather pattern mapping, wildfire monitoring, and geophysical surveying. More examples of applications can be found in Ref. 1 and Ref. 2.

The main components of the PDF architecture are shown in Figure 1. Vehicle, payload and remote sensors continuously collect data about the environment and monitored systems of interest. Using this data, the sensor processing pipeline performs feature extraction to update a dynamic database representing the aggregate knowledge of its environment. The database contains models and constraints for the vehicle, sensor, environment, and monitored system. The outer layer controller queries this database to perform mission-level decision-making, planning, and scheduling, producing mission-level commands such as desired targets, mission objective functions, and constraint and obstacle definitions. Based on these commands, the middle layer controller generates trajectories that optimize the given objectives while satisfying the constraints. Finally, to close the loop, the inner layer controls the vehicle such that the given trajectory is closely followed.

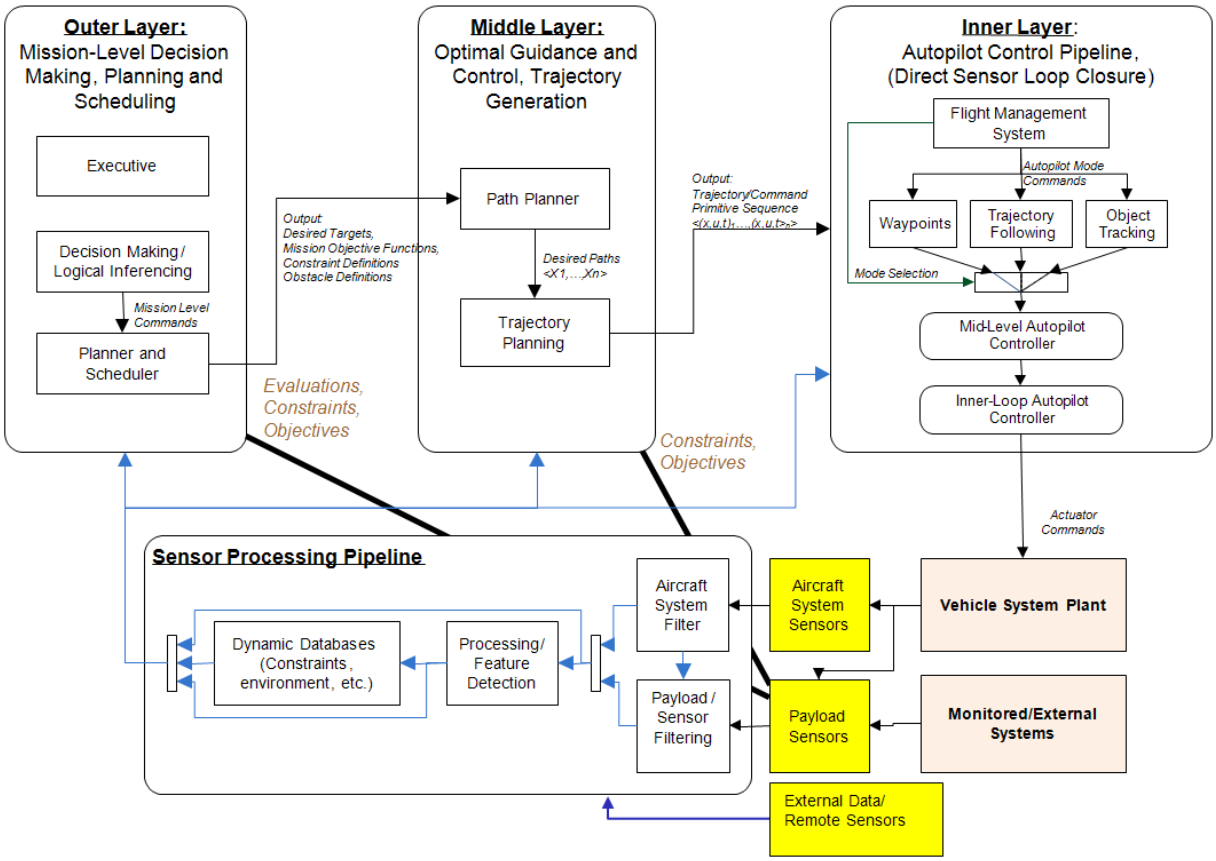

Figure 1. Block Diagram of Payload-Directed Flight Architecture.

In previous PDF work, middle-layer control capabilities were demonstrated by an algorithm known as NAETGEN, discussed in Ref. 4. NAETGEN uses Random Search Trees to produce pseudo-optimal trajectories that maximize mission objectives while satisfying mission and aircraft dynamic constraints. Reflection simulation of the algorithm applied to a wildfire monitoring example is shown in Figure 2.

Figure 2. Simulation of a UAV monitoring a wildfire using a body-fixed imager (left), and NAETGEN, a trajectory generation method based on Random Search Trees (right).

Inner-layer control is responsible for controlling the vehicle at the actuator level to accurately follow the trajectory specified by the middle layer controller. This is a non-trivial task that requires aggressive non-linear flight control in multiple flight regimes, and the topic remains an open research challenge today. Towards this end, researchers Adami et al. are exploring a promising solution using Trajectory Linearization Control. Please refer to Ref. 5 for further details.

B. Target Mission Concept

As part of a three-way collaboration between researchers from NASA, Carnegie Mellon Innovations Laboratory (CMIL), and United States Geological Survey (USGS), the PDF team is investigating, implementing, and testing PDF concepts in geophysical applications. Such close collaborations not only allow scientists to play a greater direct role in complex geologic data collection and mission planning, but also allow intelligent systems researchers to see first-hand how scientists will work with and use the systems. This leads to greater mutual understanding of objectives and features, ultimately leading to better system design and avoidance of many problems that arise from isolated development.

The target mission concept is depicted in Figure 3. First, the scientists choose a location and the subject to be studied. The subject can be any geologically interesting phenomena such as fault zones, geothermal deposits, or lava flows. Subsequently, sensors that are best suited to characterize this subject are mounted to the host platform for deployment. The vehicle computer is pre-loaded with mission objectives and a priori information about its environment, such as sensor models, vehicle dynamics, terrain models, meteorological information, and phenomena-specific models. During the survey, onboard software combines the various sensor and navigation information to construct a unified understanding of its environment and the phenomenon of interest. This representation is constantly updated as new information arrives, and provides a central and compact means to store the acquired information. By querying this knowledge base, the intelligent payload-directed controller plans and executes trajectories that optimize mission objectives.

For example, if the mission objectives were to fully characterize a phenomenon, PDF control may execute trajectories that balance gathering higher resolution data from scientifically interesting regions with the exploration of unknown territories. In this manner, with repeated knowledge update and continuous real-time trajectory revision, the autonomy greatly enhances scientific return of the collected data. Furthermore, as the survey progresses, information collected thus far is distributed via servers to off-site scientists and the world-wide web community, consequently enabling virtual mission participation and real-time analysis and feedback. Such feedback may be invaluable, for example, in evaluating the quality of the returned data, and in planning the next high-level steps in the mission.

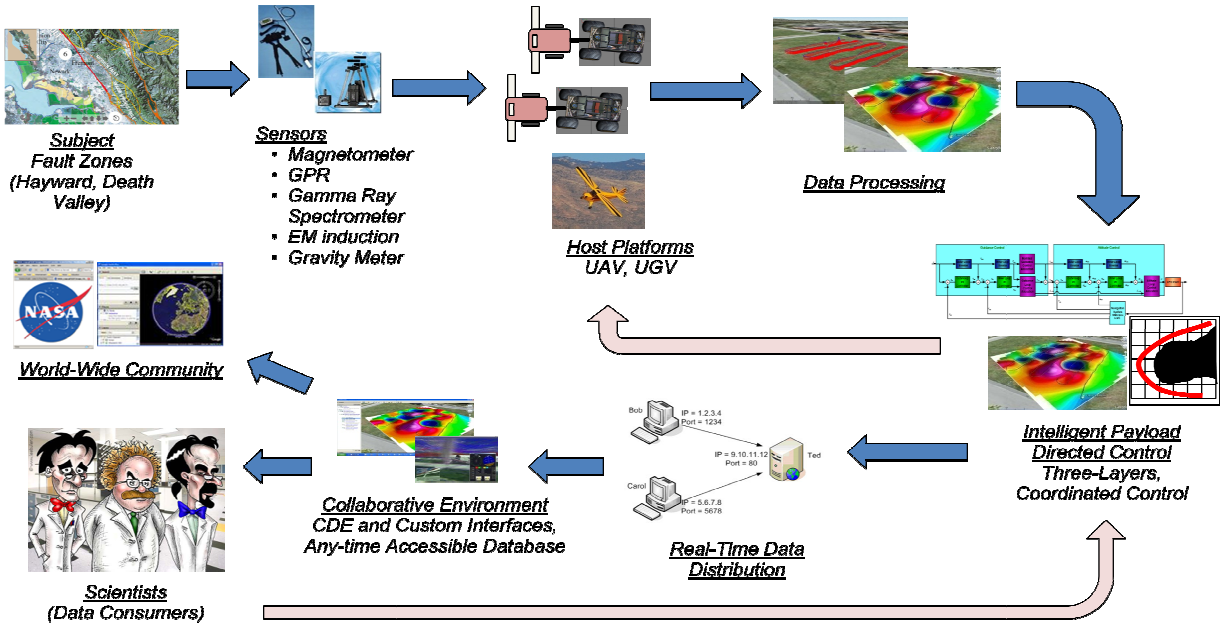

Figure 3. Concept diagram of an intelligent geological survey mission.

III. Experimental Setup

Based on the target mission concept discussed above, an experimental system employing magnetometers and their processing algorithms was created to serve as the basis for answering the key questions of this study. The system is detailed in this section.

A. Magnetometers

Magnetometers are passive, relatively small, and easy to deploy sensors that are able to delineate magnetic rock bodies. Since the magnetic signature of a magnetic body decreases with the cube of the distance, objects that are closer to the sensor dominate the signal, typically higher frequencies. Ground, or low-flying (300 m) aerial, magnetic surveys are typically conducted over local areas of interest, such as individual valleys. These surveys focus on characterizing short-wavelength magnetic signals caused by natural features and man-made objects, such as faults, stream channels, geothermal and mineral deposits, tunnels, and unexploded ordinance (UXO). At higher elevations, aerial magnetic surveys are flown over larger areas and focus on characterizing the longer wavelength magnetic signals caused by rock bodies a few kilometers or more below the earth's surface.

A Geometrics G-858/G magnetometer system, shown in Figure 4 with a single magnetometer, was used for this PDF investigation. The full system consists of two magnetometers and a console. Specifications are shown in Table 1. The sensor payload for future aerial surveys would be the Geometrics G-822 Marine Magnetometer, a heavier but more accurate sensor package, not described here.

Figure 4. Photograph of a Geometrics G-858 Magnetometer (Image source: Geometrics Inc.)

Table 1. Geometrics G-858 Specifications

Manufacturer	Geometrics
Make	G-858/G
Operating Range	20,000 to 100,000 nT
Sensitivity	0.01 nT at 1.0 sec cycle rate (SX=0.051nT)
Output	RS-232, 115.2KBaud
Weight, Gradiometer/Console	0.32 KG each / 1.6 KG
Weight, Battery/Staff	2.6 KG each/ 0.9 KG
Power Supply	24 VDC / 5.0Ah supplied
Sensor Dimensions	6 cm x 15 cm, 340 g
Console Dimensions	15 cm x 8 cm x 28 cm, 1.6 kg
Operating Temp	-15°C to +50°C
Shock	Drop 3 ft on a hard surface without damage

B. Host Platform Technologies

An unmanned ground vehicle (UGV) was used in the experimental setup. However, unmanned aerial vehicles (UAV) were studied as possible host platforms as well.

1) Autonomous Ground Vehicle Technology

The ground vehicle used was the NASA MAX5A UGV. The MAX5A is a compact four-wheel drive rover, with overall dimensions of approximately 46 cm x 38 cm x 48 cm (18.1" x 15.0" x 18.9"). Total weight is approximately 10 kg (22 lbs), and payload capacity is 5 kg (11 lbs). Its top speed ranges from 2 – 5 m/s (6.6-16.4 ft/s) depending on payload weight and battery capacity. The onboard computer is a Mini-ITX form-factor Intel Centrino 1.6 GHz Pentium-M single-board computer. Communication links were provided by IEEE 802.11g wireless devices as well

as 900 MHz spread spectrum radio modems. Localization and orientation estimation were provided by an onboard Athena GS111m inertial navigation system (INS), and a NovAtel OEM4-G2 Differential GPS (DGPS). The combined system gives geo-location accuracies of better than 1 m. Figure 5 shows photographs of the MAX5A UGV before and after the installation of the magnetometer system. Additional information about the UGV can be found in Ref. 9.

Figure 5. Photograph of MAX5A in standard (left) and modified (right) configurations.

2) Autonomous Aerial Vehicle Technology

Two candidates for aerial host platforms are the NASA Exploration Aerial Vehicle (EAV) and the NASA eXperimental Sensor-Controlled Aerial Vehicle (X-SCAV). Specifications of both these vehicles are shown in Figure 6.

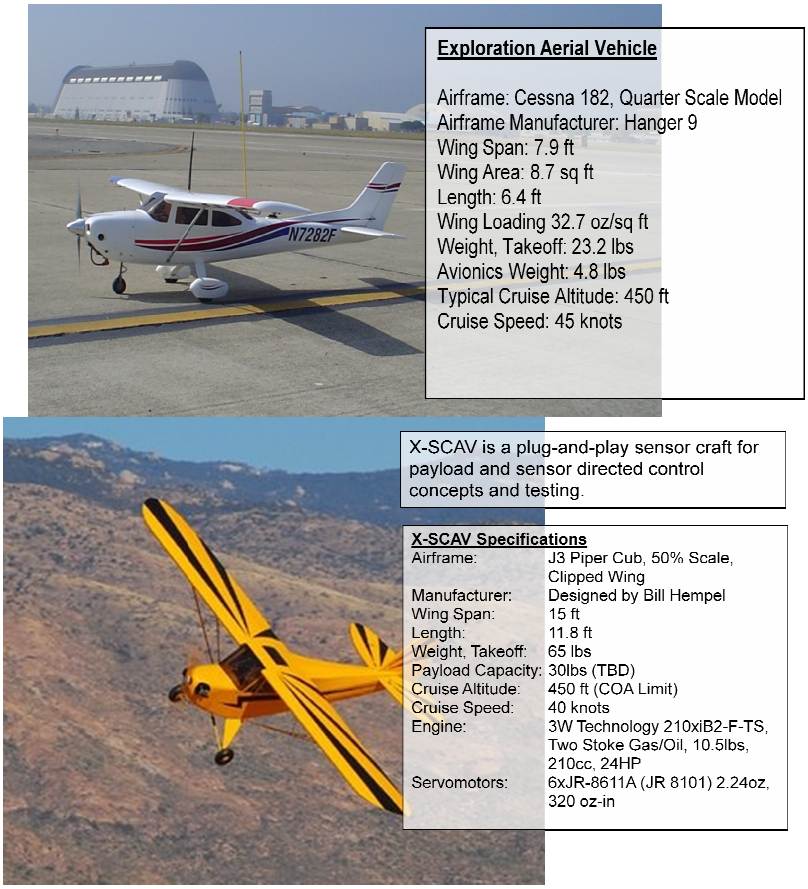

Figure 6. A listing of NASA EAV (top), and X-SCAV (bottom) specifications

In particular, the X-SCAV is the best-suited for the aerial magnetic surveys because of its larger size and greater payload capacity. In addition, the vehicle is constructed almost entirely from non-magnetic materials. The bulk of the frame is wood, with the exception of the metal bars of the landing gear. The skin coating and cowling are made of plastic and fiberglass, respectively. Furthermore, because of the extended wingspan, the magnetometers can be placed up to seven feet away from the main magnetic source (the engine) when installed along either wingtip. Additional information about the X-SCAV can be found in Ref. 4.

3) Software

MAX, EAV and X-SCAV run the NASA Reflection software architecture, which is a real-time component-based plug-and-play architecture for the development of embedded vehicle systems. The Reflection system facilitates the rapid prototyping, development, and deployment of research software for field testing on real vehicle systems, reducing costs by providing reconfiguration capabilities and tools for rapid prototyping, while minimizing risk to the platform by providing an extensive automated testing framework. Furthermore, the software provides many core autonomous vehicle capabilities such as waypoint navigation, sensor fusion, and low-level actuator control. More details on Reflection can be found in Ref. 13. In this feasibility study, autonomous waypoint navigation was used in place of the three-layer payload-directed control, which is still in development.

4) Hardware and Software Integration

An overview of the complete system configured for performing magnetic surveys is shown in Figure 7. The system has three main components: a map server, the UGV ground station, and the combined sensor-UGV system. The ground station is a fast dual-core laptop with a large screen for displaying the map visualizations and UGV control interface. In these experiments, the computationally intensive minimum curvature algorithm was run on the ground station as a low-priority thread. However, to perform a payload-directed survey, the processing would need to be executed on the vehicle.

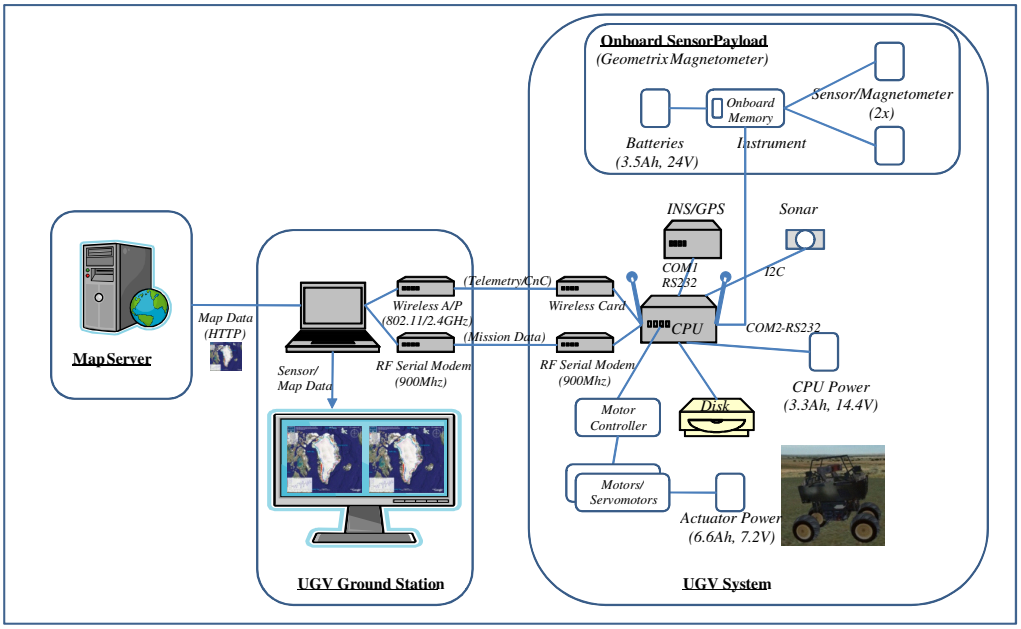

Figure 7. Overview of UGV survey system.

The total weight of the magnetometer sensor payload was about 8.34 kg, or 18.4 pounds. This exceeded the original specifications for the MAX5A. The MAX5A was reconfigured with stiffer suspension, and the stereo camera head was removed, as shown in Figure 5. Extensive testing of the UGV suspension and battery capacity under the increased load was performed before deployment. Bumper balls were added to prevent damage to sensors in the case of the UGV tilting too far on either side. The overall throttle level was reduced to handle small mounds and turns. Occasional motor overheating problems were observed on some grass surveys, because of the overweight

payload. Moreover, the small wheelbase of the MAX5A placed limitations on the survey terrain. For these reasons, a larger, more payload-capable ground vehicle is planned for future development.

The MAX5A contains many potential sources of magnetic interference including brushless motors, various electronics, NiMH and lead acid batteries, and a metallic and carbon fiber chassis. Requirements for the mounting of the magnetometers included maintaining a distance of approximately one meter above the ground, and as far as possible from the magnetic field from the UGV's electronics and motors. Layers of magnetic shielding film, more commonly known as mu-metal, were wrapped around the front motor to direct its magnetic field away from the sensors. Electro-magnetic interference was observed to affect the DGPS packet drop rate, which ultimately led to the DGPS antenna being elevated above the main chassis.

The magnetometer sensors were mounted on the end of a forward-protruding pole, and the magnetometer console and batteries were rigidly mounted to the back and sides of the UGV via mounting brackets. The mounting configuration is shown in Figure 8. Mounting one of the magnetometers horizontally was intended to provide a source of different magnetometer information. However, it was later found that that was a poor choice because the sensor dead-zones caused the channel to exhibit dropouts at certain headings.

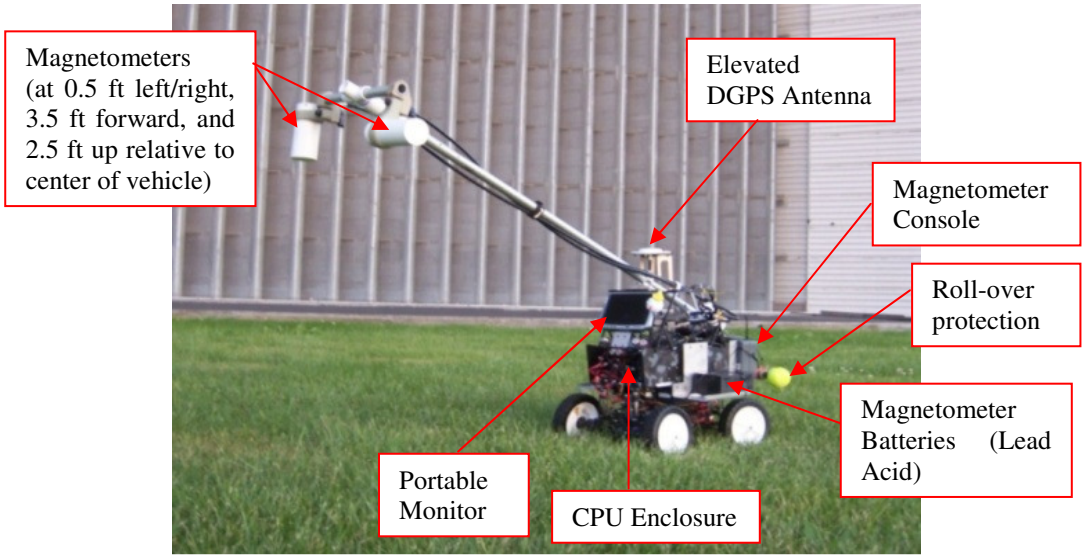

Figure 8. MAX5A configuration details.

C. Magnetic Sensor Processing Algorithms

One of the main difficulties in performing real-time control around payload sensors is processing the data in a timely fashion. The NASA and Carnegie Mellon team developed real-time software to geo-locate magnetometer sensor data using a suite of onboard vehicle sensors. The software processes the data stream to produce and update magnetic surface maps that can be utilized to optimize vehicle trajectories in real-time. This was done in a series of steps, which are outlined in Figure 9 below.

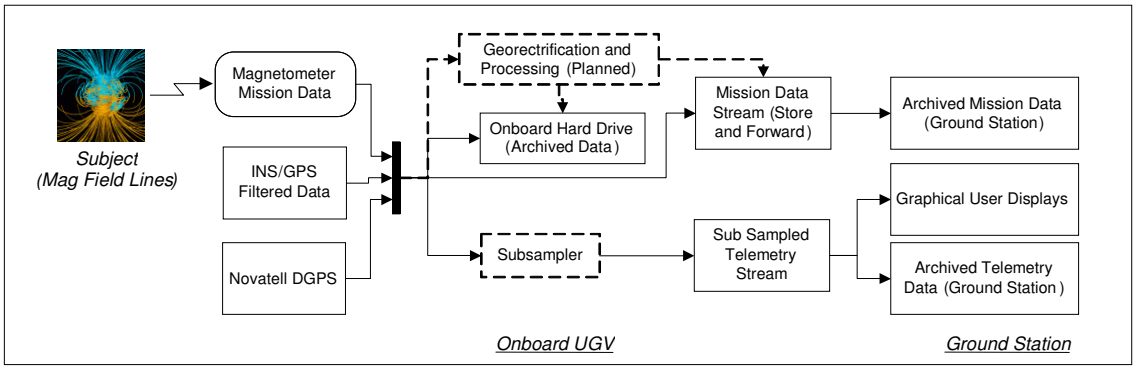

Figure 9. Sensor dataflow block diagram

For each survey, initial setup involved loading the map and GPS coordinates of the survey location into the Reflection system, and selecting a series of waypoints in a grid survey pattern using the map display as shown in Figure 10. The GPS coordinates for the four corners of the survey pattern were then used to determine the size of the grid storage structure on the ground station. The grid was used to store, interpolate, and display in real-time the magnetometer readings during the survey. Assuming the UGV would traverse successive rows in a left-to-right, then right-to-left manner, with about ten feet between each leg, the grid size was chosen such that grid spacing would be no larger than half of ten feet, or five feet. This was chosen to ensure sufficient sampling density, while optimizing algorithm run time.

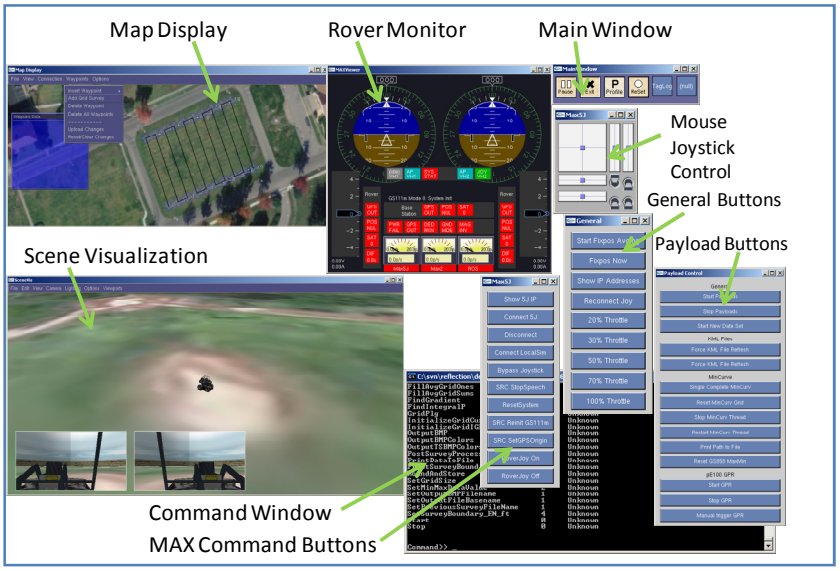

Figure 10. Ground station Reflection GUI for geophysical surveys.

The Geometrics magnetometer console relayed sensor data via RS-232 serial connection at 115.2 kbps to the MAX computer. The software module on the UGV checked, processed, and logged the data at a maximum sampling rate of 50Hz. Furthermore, the sensor data was transmitted to the ground station each time the UGV traversed a minimum distance. This threshold was set to four feet on the basis of the minimum spacing of the grid storage structure. If the UGV was not moving, no new sensor data would be transmitted, but position, orientation, and control information would continue to be transmitted back to the ground station at 10 Hz.

Magnetometer data pre-processing procedures were based loosely on Ref. 11. Diurnal corrections and map projection corrections were not implemented at this stage as surveys were carried out in under an hour, and over a small area. These corrections would be included in aerial surveys. Dropouts in magnetometer data were received as zeros and filtered out as anomalous noise. Grid values were initialized at the average magnetic field (IGRF) of the area, as given by the National Geophysical Data Center (NGDC) in Ref. 12.

On the ground station, sensor data were interpolated into the grid storage, as required by the implementation of the minimum curvature interpolation algorithm, using the formulas:

$$grid[i] = round\left(\frac{gridSizeI - 1}{x_{max} - x_{min}}(x - x_{min})\right) \quad grid[j] = round\left(\frac{gridSizeJ - 1}{y_{max} - y_{min}}(y - y_{min})\right) \tag{1}$$

where x_{max}, x_{min}, y_{max}, and y_{min} were the GPS coordinates for the four corners of the survey area. Points outside these GPS bounds were not logged in the grid. The transformation is illustrated in Figure 11.

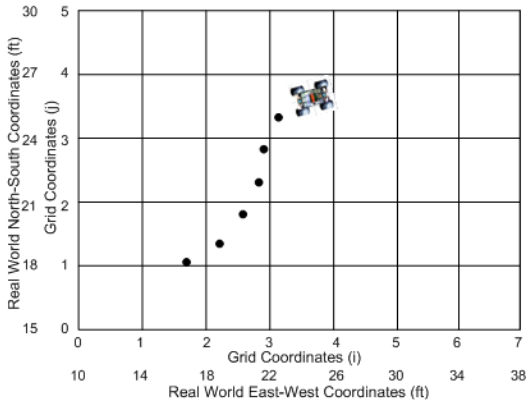

Figure 11. Mapping datapoints to internal grid. Measurements made in the same grid coordinates are averaged.

Data values for the grid points where no sensor data was available were interpolated using a minimum curvature two-dimensional spline-fitting method. This method of using minimum curvature to produce contour plots was introduced by Briggs in 1974, and versions of Briggs' method are in widespread use in the Earth Science community. A detailed description of the algorithm, along with the equations, can be found in Ref. 6. Our algorithm was based on both the Briggs algorithm (Ref. 6) and in-house FORTRAN code written by the USGS.

The algorithm, which was based on a series of difference equations, was implemented as a Reflection module with additional data protection features. Points collocated with measured data were marked as full and no longer recalculated in ensuing iterations. The grid was locked by a mutex while the algorithm ran to prevent the grid values from being modified during calculations. This emulated the original post-processing usage of the algorithm, in which the algorithm, if the grid points are sufficiently close, should converge after approximately one hundred iterations (Ref. 7). The data sequence diagram for our software is shown below in Figure 12:

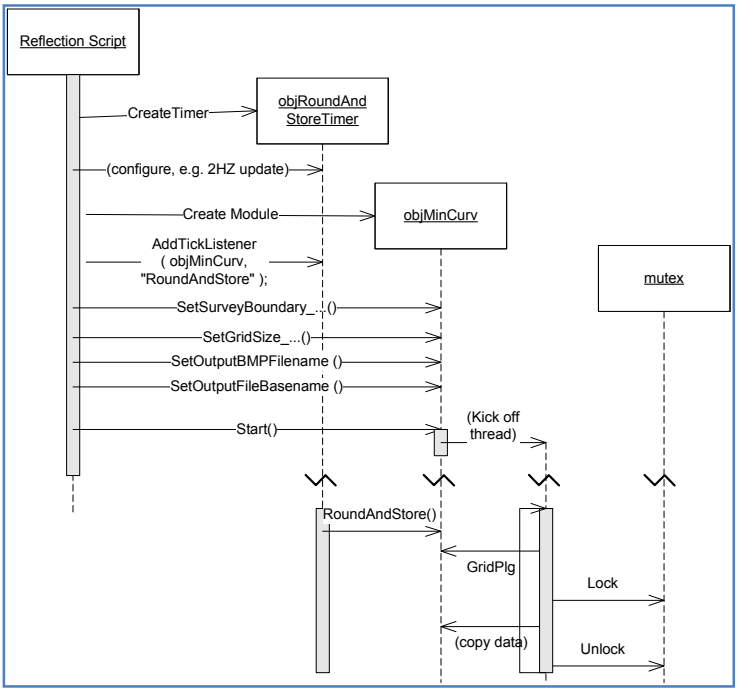

Figure 12. Reflection data sequence diagram.

Commands to pause, reset, and restart the algorithm were also available as part of the ground station display. In one early trial, two researchers approached the UGV to change the batteries, and their presence showed up on the

grid as a magnetic anomaly. Adding a "pause" button allowed such issues to be handled appropriately. Functions for finding the gradient values and integrating between points on the grid were also written but were not used in these surveys.

A number of improvements remain to be implemented. Instead of averaging data values that map to the same point on the grid, weighted averages or fitted paraboloids could result in faster convergence, as described in Ref. 7. Also, edge effects were present in the data, as a result of the assumption used for the minimum curvature algorithm that edges are free, extending into planar surfaces. These effects may be eliminated by implementing the splines with tension technique extension to minimum curvature described in Ref. 10, in which the edges are forced to flatten. For these surveys, edge effects were minimized slightly by choosing slightly larger grid sizes and initializing grid values to the IGRF value.

D. Real-time Communication and Data Distribution

The NASA and Carnegie Mellon team developed software to distribute processed payload sensor data streams in real-time to scientists around the world. After processing the sensor data, a software module generates a Google Earth-compatible file that gets distributed via the world-wide web. Scientists using Google Earth software would be able to see updating geo-referenced magnetic map overlays as the mission progressed.

In these experimental trials, the files were only distributed locally to allow geo-scientists in the field to visualize the magnetic field maps as they were updated in real-time. Based on instant feedback from these geo-scientists, the survey team was able to quickly adapt the survey to focus on 'hot-spot' locations.

IV. Experimental Results

In this section, we present the results of our feasibility study, and discuss each of the questions posed in Section I.

A. Using Magnetometer Systems with Autonomous Platforms

In the experimental setup, a Geometrics G-858/G magnetometer system was successfully integrated with a MAX5A UGV, and demonstrated real-time autonom -96.190 llection, sensor fusion, data distribution, and vehicle control. Furthermore, since the EAV and X-SCAV run similar hardware and software to the MAX5A, integration with UAV's would be done in similar fashion.

Experiments to assess the magnetic interference from the host vehicles were also performed. For the UGV, laboratory tests showed that magnetic interference effects from the front motor were apparent at 3 feet from the UGV. Several layers of magnetic shielding film were subsequently used to wrap the front motor and redirect the field. After the shielding was applied, the effects of the motor became small relative to the sensor drift. Magnetic interference from the CPU box was negligible.

For the aircraft, testing of the electromagnetic field effects of UAV engine, avionics, and servos were carried out by Geometrics Inc. at the Moffett Field Compass Rose, where the ground is clear of magnetic material. These tests showed that the EAV engine, when running, had a fairly steady oscillating signature with an amplitude of 2 nT, and that there was a 20 nT difference between the engine on and off from a distance of about three feet. This is shown in Figure 13. Servo deflections had a very minute effect, changing the gradient by less than 1 nT, as shown in Figure 14 (Ref. 14). Avionics did not have a measurable effect.

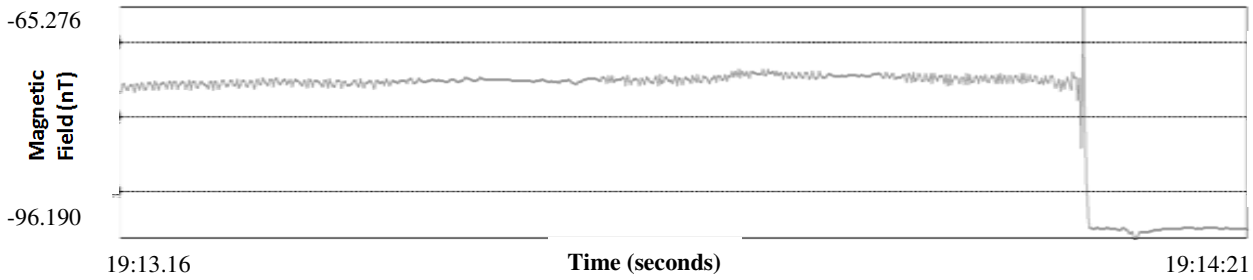

Figure 13. Magnetic field signature of EAV engine. The engine is initially running and turned off approximately 50 seconds into the experiment.

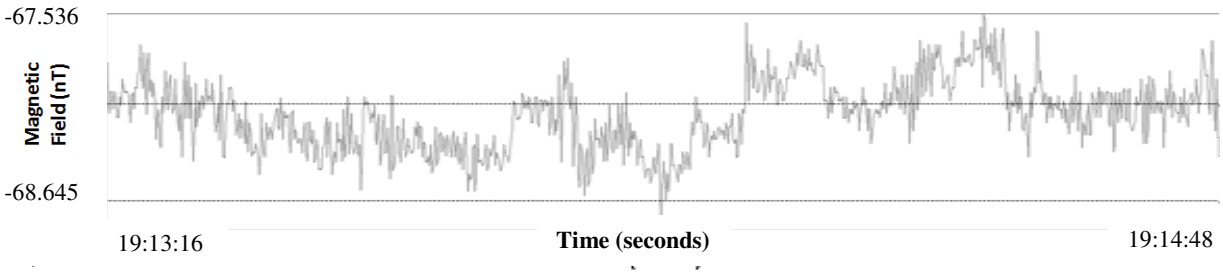

Figure 14. Magnetic Field Signature of a series of servo deflections.

B. Using Magnetometer Data In Feedback Control

Below are two examples of real-time visualization images generated over the course of two surveys. Figure 15 shows a sequence of five snapshots displaying the contents of the minimum curvature internal grid at those instants during the survey. The UGV is traversing a grid pattern trajectory from the bottom right corner to the middle of the left side, and the snapshots show the developing interpolated image as the UGV completes the survey. The second sequence (Figure 16), also a composite of snapshots, shows the developing interpolated magnetic data as the UGV traverses a northwest to southeast grid pattern. Edge effects, artifacts arising from the minimum curvature algorithm, can be seen as the large purple regions along the sides of the snapshots.

The range of the color spectrum in the images was normalized to the current maximum and minimum recorded sensor values. The rationale was to maintain maximum color contrast in the real-time display during the survey. As new maximum and minimum values were set, the color range would shift, as is evident in the second sequence below. This is a visualization preference that can be changed easily. In general, magnetometer values remained in a range between 30000 and 60000 nT, with standard deviation per survey of about 3000 nT. The data was parsed, processed, and overlaid in Google Earth for real-time visualization. The magnetic target can be seen as a developing linear feature that runs top-left to bottom-right in Figure 15 and across the outfield in Figure 16.

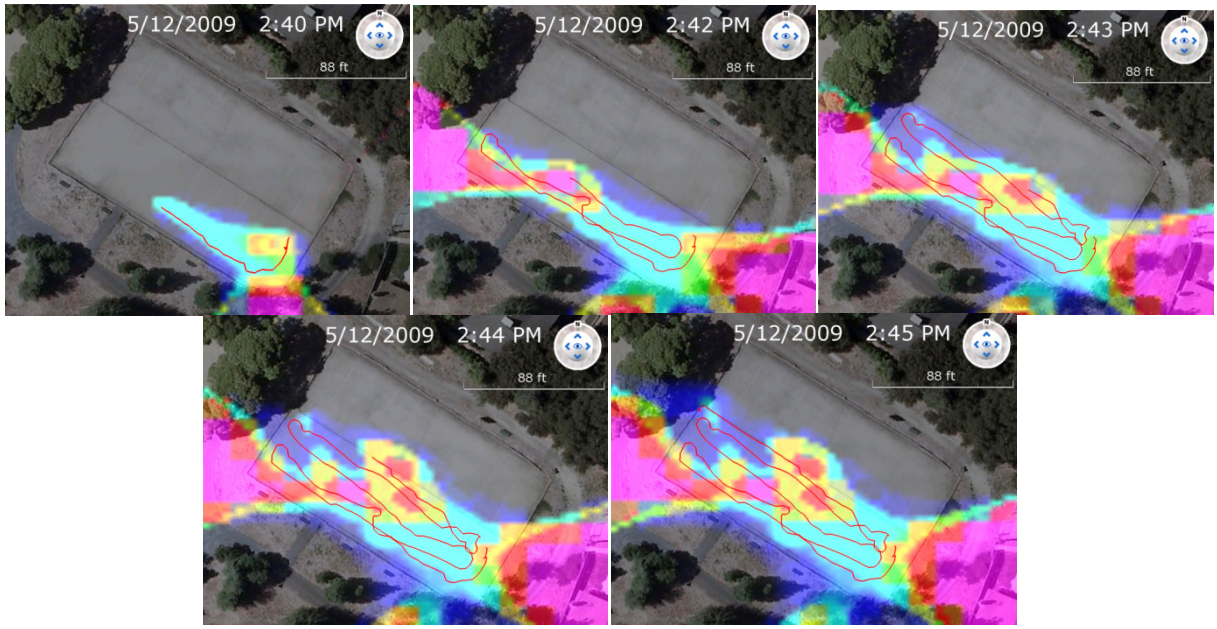

Figure 15. Example of a sequence of real-time visualization images from a survey. The vehicle trajectory is shown in red. Color spectrum is determined by minimum and maximum recorded sensor measurements.

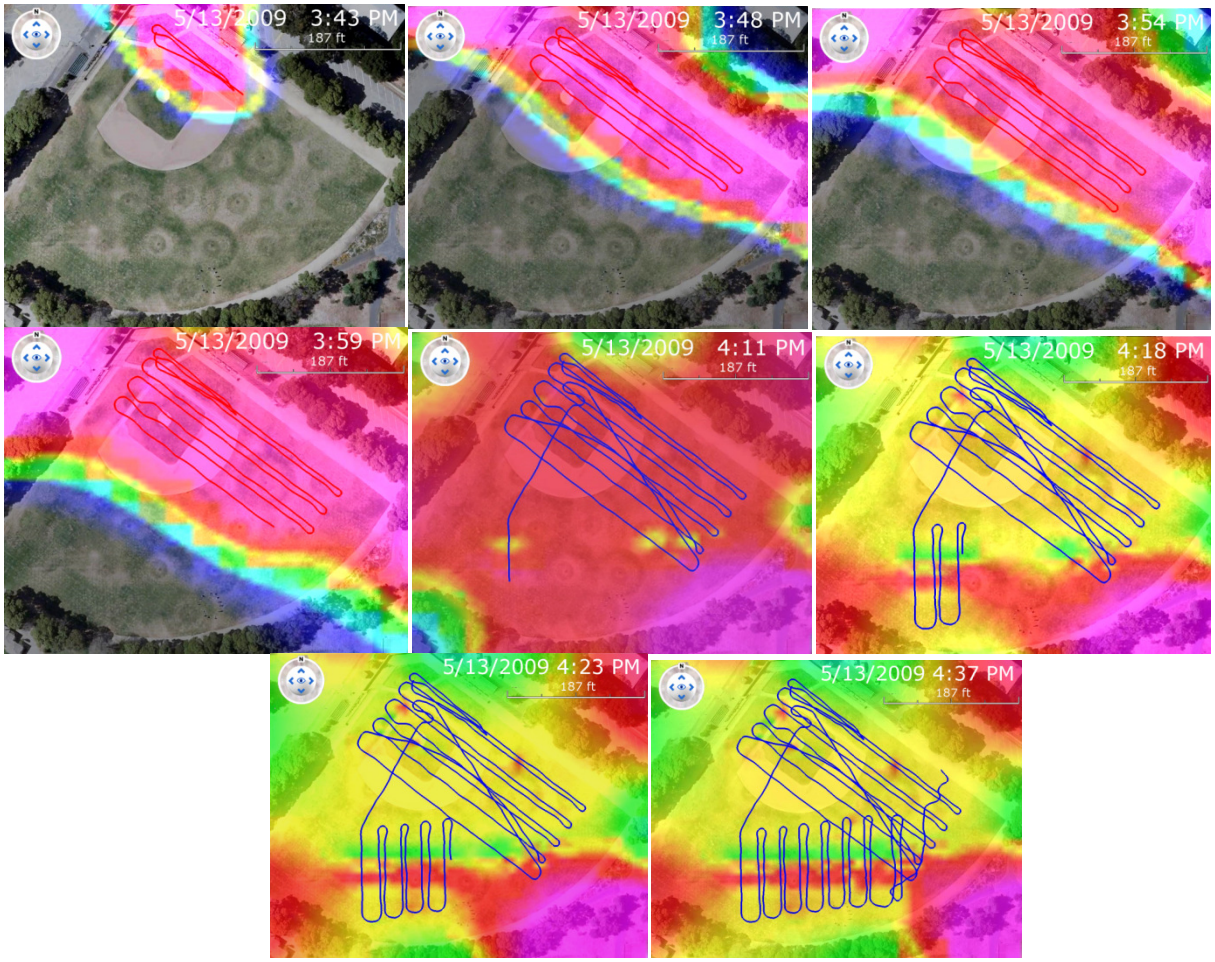

Figure 16. Example of a sequence of real-time visualization images from a survey. The vehicle trajectory is shown in red, then blue. Color spectrum is determined by minimum and maximum recorded measurements.

In this study, we successfully implemented a magnetic sensor processing algorithm that would be suitable for sensor feedback. Not only did the minimum curvature method provide processing and modeling of magnetic data, it also did this in real-time. In fact, the algorithm could be executed on a grid of size 128x128 at about 421 iterations per second on a single dedicated processor. These speeds should be more than adequate for most real-time control purposes.

Due to the complexity of magnetic data modeling, the simplified model that the minimum curvature technique provides may not be sufficient to accurately model the phenomenon of interest. In these cases, human interpretation or more sophisticated algorithms and models may be required.

C. Using the Experimental System to Correctly Identify and Map Magnetic Features

To evaluate the capabilities of the system, the UGV was deployed on three occasions. The results of those deployments demonstrate the system's ability to characterize magnetic features.

1) A Technology Validation at Flood Park

The first deployment tested the UGV by surveying a known man-made structure, an iron-encased aqueduct approximately 2 m in diameter that passes beneath the baseball field and bocce ball court at Flood Park in Menlo Park, California. By considering a known subject, this deployment served not only as a technology demonstrator, but also to provide a clear baseline for the survey system.

At Flood Park, two autonomous surveys were performed across the baseball field and bocce ball court. The surveys tested both the real-time generation and display of the continuously evolving magnetic surface map, as well as the system's ability to characterize the phenomenon. In both regards, the deployment was a success. Not only was the magnetic signature of the aqueduct prominently visible, the processing algorithms were also able to, in real-

time, compute and visualize contour plots of the study area. The magnetic feature caused by the magnetic field of the aqueduct can be clearly seen in Figure 17 as a linear feature running east to west.

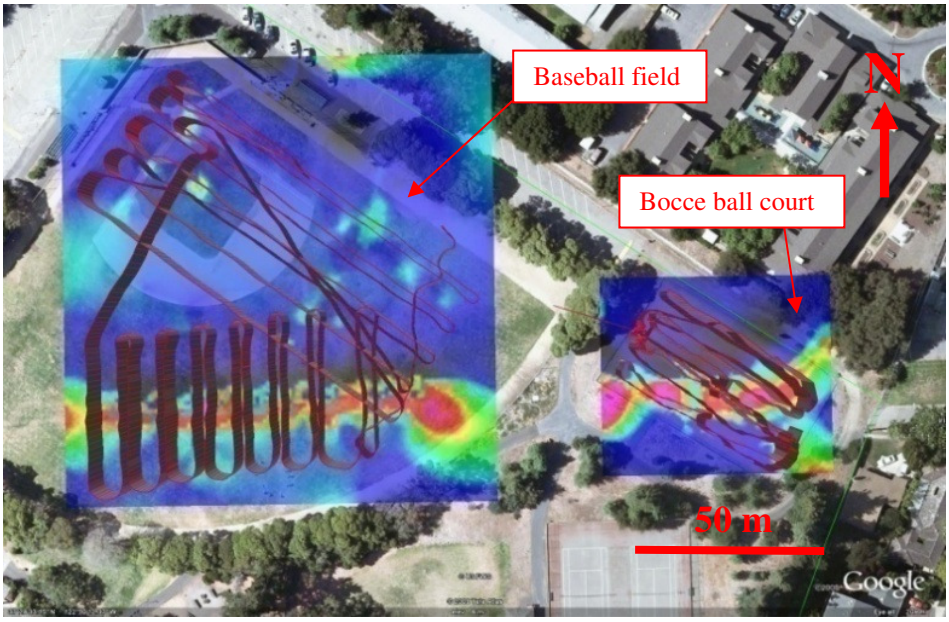

Figure 17. A minimum curvature visualization image of two autonomous surveys performed at Flood Park. The aqueduct running beneath is clearly visible running horizontally across the outfield of the baseball field, and beneath the bocce ball court.

In the bocce ball court survey, there was an unknown source of electro-magnetic interference (possibly from overhead power lines) that caused intermittent DGPS fluctuations, as well as a few anomalous magnetometer measurements. Some of these effects are manifested as discontinuities in the linear magnetic feature of the aqueduct. Uneven terrain, such as potholes and mounds caused maneuvering problems because of the UGV's small wheel size.

2) An Active Fault Zone Investigation at Ohlone College

In a second deployment, the UGV surveyed a baseball field at Ohlone College, located in Fremont, California. The target of interest was a possible active fault beneath the baseball field. A previous shallow seismic reflection survey across the area (M. Rymer, written communication, 2009) imaged anomalous subsurface soil and rock, possibly, but not conclusively, indicative of an active fault. Faults often produce linear magnetic anomalies because tectonic movement on the faults has juxtaposed lithologies with differing magnetic properties. The UGV was deployed to test for evidence of a fault using the real-time generation and display of the magnetic field map. As in the first deployment, two individual surveys were run across the baseball field. However, unlike the previous survey, which identified a known target, the real-time magnetic surface maps, as shown in Figure 18, did not reveal any obvious subsurface magnetic targets.

The real-time data processing workflow does not yet include corrections for diurnal magnetic effect and survey leveling, so the final processing of the data is still pending analysis by the USGS. However, the generated magnetic surface map is a strong indicator that there is no evidence of linear magnetic features within the survey area; if there is a fault, it does not appear to juxtapose materials with differing magnetic properties.

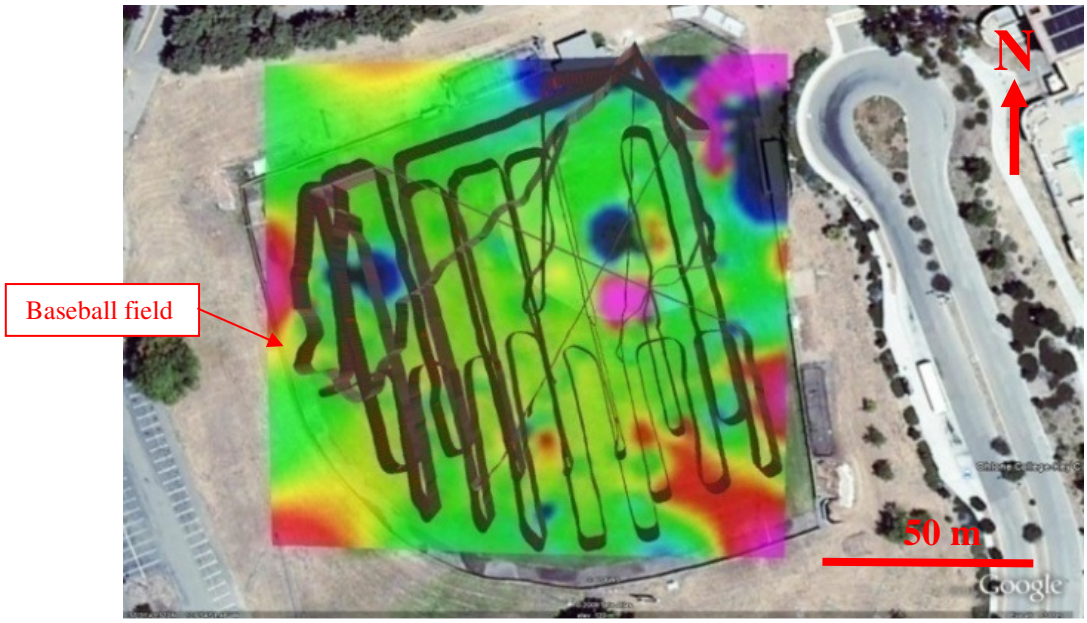

Figure 18. A minimum curvature visualization image of an autonomous survey performed at Ohlone College in search for fault lines.

3) A Murder Investigation at Alviso

In a third deployment, the NASA Payload-Directed Flight research team, again in collaboration with the USGS in Menlo Park and CMIL, provided assistance to the County of Santa Clara's District Attorney's Office in California in a cold case murder investigation. This deployment was not part of the experimental plan, but provided a good opportunity to push the limits and see how well the system would perform in a challenging environment. The team deployed the instrumented autonomous ground vehicle to perform magnetic surveys of an old junk yard in Alviso, California, looking for buried material evidence, which included metal car parts. The application of research algorithms provided the means to collect data and locate the buried material evidence, which was subsequently excavated. Photographs of the deployment are shown in Figure 19.

Figure 19. USGS personnel carrying the NASA instrumented MAX UGV during Alviso survey (left). Santa Clara County DA Office personnel inspect a 'hotspot' (right).

A critical element of this deployment was the need for rapid data collection and modeling. Legal constraints allowed for only a brief field investigation (one day and one follow-up day, if necessary), and the modeling needed to be completed within two weeks. The new field techniques developed by this joint NASA-USGS effort allowed for real-time data download, processing, and preliminary analysis. This was key to the investigation, because it allowed USGS scientists to obtain preliminary results during the field session, when critical access to the site was available and investigators were on-site to address problems and carry out immediate follow-on investigations.

Crews spent the initial field time removing surface debris from the surface, which consisted of various metal and non-metal construction detritus such as small lengths of reinforcement bars, bolts, boards with nails, lengths of chain, cyclone fencing, etc. Despite removal of the surface debris, it was obvious that the terrain would be too cluttered for the UGV to traverse autonomously. As a result, it was decided that the UGV be mounted on a wooden

board and hand-carried across the study area in a row-by-row pattern. The site was surveyed in less than 30 minutes, so the diurnal correction was assumed to be negligible. As the magnetic data were received it was processed at the base station and a real-time magnetic map was produced as the survey progressed, allowing feedback from the base crew to the survey crew.

At the completion of the first survey the USGS identified areas of interest A, B, and C, shown in Figure 20 based on the locally high magnetic field, and a second, more detailed survey, shown in Figure 21 was conducted to better delineate the anomalies detected by the first survey. The second survey revealed three areas of interest common to the first survey, and one area from the first survey that was initially thought to be significant was revealed to be a surveying artifact. At the completion of the second survey the magnetic map delineating the three areas of interest, based on the magnetic data combined with information from local investigators, was given to investigative team.

Offsite, following the survey, the USGS modeled the magnetic anomalies as highly susceptible bodies (> 1 SI), consistent with large manmade objects with a high iron content. Two-dimensional cross-section modeling across each of the three anomalies indicated magnetic objects at approximately 2 meters depth. The models were given to investigators to help focus their efforts.

Three pits were dug by the investigators, each several meters across and between two and three meters deep. The USGS was not present during the exhumation, and the precise location and amount of debris was not recorded. However, the investigators informed the USGS that several parts from an automobile were discovered in location A (Figure 20). Only minor amounts of debris were found at locations B and C (Figure 20). In general the amount of debris discovered was smaller in volume than the modeling predicted, suggesting the modeling used too low a value of magnetic susceptibility for the manmade parts. However, the location and relative amounts of manmade parts were consistent with the modeling.

The excavation eventually led to the successful conclusion of this 18-year old case.

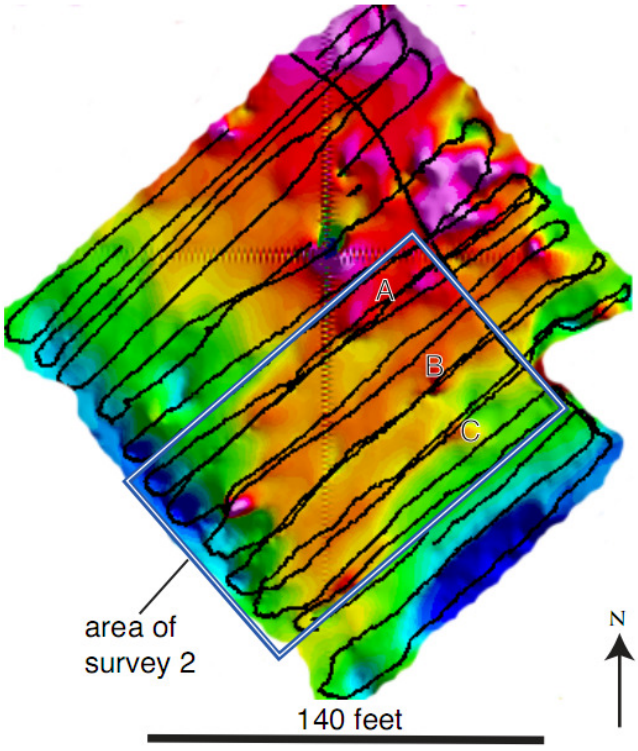

Figure 20. Post-processed map of magnetometer data of the first Alviso survey.
Hotspots A, B, and C were identified and a second survey was performed.

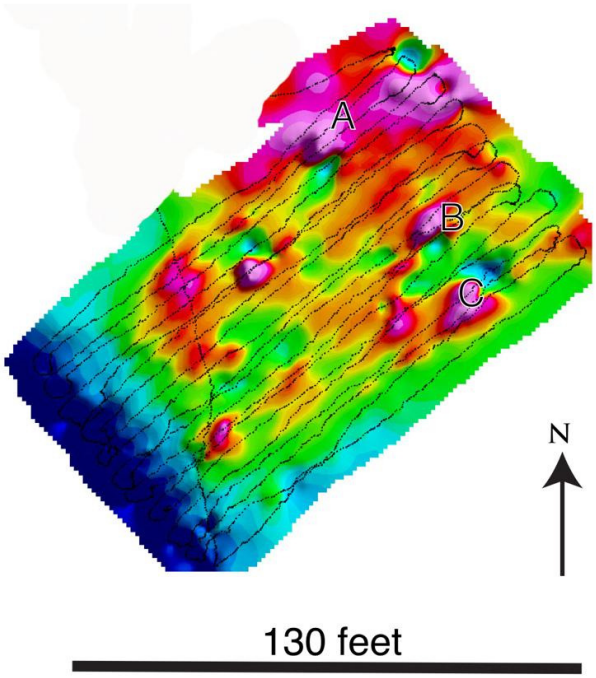

Figure 21. Post-processed map of magnetometer data of the second Alviso survey.
Hotspots A, B, and C were identified and subsequenly excavated.

V. Conclusions

In this study, an experimental system was developed and deployed to evaluate the feasibility of performing payload-directed geophysical magnetic surveys. First, a magnetometer system was integrated with an unmanned vehicle and demonstrated real-time autonomous data collection, sensor fusion, data distribution, and vehicle control. Secondly, processing and modeling of magnetic data were demonstrated to be possible in real-time. Finally, the experimental system demonstrated the ability to correctly map real-world magnetic features.

Preliminary results from experiments and deployments have shown promise in the feasibility of intelligent survey control. In particular, this approach was demonstrated to be especially compelling in geophysical surveys where exhaustive surveys are impractical, such as those where coverage is large and areas of interest are unknown.

Several challenges were observed during the investigation. First, noise from ground and aerial vehicle magnetic sources was identified to be significant and required mitigation action to keep the host platform from corrupting sensor data. Secondly, the use of a small UGV as a host platform presented many limitations, including carrying capacity (which caused overheating motors), real-estate (clearance to interference sources), battery power, range, and ability to traverse uneven terrain (such as potholes, protrusions). Larger UGV's, on the order of an adult bicycle or golf cart, as well as obstacle avoidance capabilities are recommend for future ground surveys. Aerial platforms were investigated, but not implemented in this experimental setup. Finally, the experimental system demonstrated only simplified data modeling and interpretation capabilities. Proper processing and understanding of the data still requires human interpretation to make sure that the autonomous decisions are correct. As a result, humans cannot be fully removed from the control loop.

Possible future work to improve the sensor processing algorithm include corrections for diurnal magnetic field, survey leveling, and gradient analysis in the magnetic data. Furthermore, a larger, more payload-capable ground vehicle is planned for future development.

Acknowledgements

The authors gratefully acknowledge NASA ARMD Subsonic Fixed Wing project for funding this work. Additionally, we give warm thanks to collaborators from USGS Menlo Park, authorities from Santa Clara District Attorney's office as well as the many summer interns and visiting scholars of the lab.

References

[1]Ippolito, C., Fladeland, M., Yeh, Y., "Applications of Payload Directed Flight," *IEEE Aerospace Conference 2009*, 7-14 March 2009, Big Sky, Montana.

[2]Beard et al., "Payload Directed Flight of Miniature Air Vehicles," *AIAA Infotech and Unmanned…Unlimited Conference,* Seattle, Washington, 6-9 Apr. 2009.

[3]Lee, R., Ippolito, C., "A Perception and Mapping Approach for Plume Detection in Payload Directed Flight," *AIAA Infotech and Unmanned…Unlimited Conference,* Seattle, Washington, 6-9 Apr. 2009.

[4]Ippolito, C., Campbell S., Yeh, Y., "A Trajectory Generation Approach for Payload Directed Flight," *AIAA Aerospace Sciences Meeting including The New Horizons Forum and Aerospace Exposition,* Orlando, Florida, 5-8 Jan. 2009.

[5]Adami, T., et al., "Six DoF Trajectory Tracking for Payload Directed Flight Using Trajectory Linearization Ccontrol," *AIAA Infotech and Unmanned…Unlimited Conference,* Seattle, Washington, 6-9 Apr. 2009.

[6]Briggs, I., "Machine contouring Using Minimum Curvature," *Geophysics,* Vol. 39, No.9, February 1974, pp. 39-48.

[7]Swain, C.J., "A Fortran IV Program for Interpolating Irregularly Spaced Data Using the Difference Equations for Minimum Curvature," *Computers & Geosciences,* Vol. 1, 1976, pp. 231-240.

[8] "Geometrics G-858 MagMapper Operation Manual 25309-OM Rev. D.," Geometrics Inc., January 2001.

[9]Ippolito, C., et al, "Polymorphic Control Reconfiguration in an Autonomous UAV with UGV Collaboration," *2008 IEEE Aerospace Conference,* Big Sky, Montana, 1-8 Mar 2008.

[10]Smith, W.H.F., Wessel, P., "Gridding with Continuous Curvature Splines in Tension," *Geophysics,* Vol. 55, No.3, March 1990, pp. 293-305.

[11]"Central West Antarctica Aeromagnetic Data Processing Procedures Website," United States Geological Survey, URL: http://pubs.usgs.gov/of/1999/ofr-99-0420/cwant_proc.html, Last update 19 Nov 1998, [cited 11 May 2009].

[12]"National Geophysical Data Center (NGDC), NOAA Satellite and Information Service," IGRF Database, Valid 1900-2015 URL: http://www.ngdc.noaa.gov/geomagmodels/IGRFWMM.jsp. [cited 11 May 2009].

[13]Ippolito C., Pisanich, G., Al-Ali, K., "Component-Based Plug-and-Play Methodologies for Embedded Technology Development," *AIAA Infotech Conference,* Arlington, Virginia, 26-29 Sep 2005.

[14]Edwards, L., Tait., G., "Scale Cessna Static Magnetic Test Report," Geometrics Inc., 3 Sep 2008.

[15]Ippolito C., Pisanich, G., Al-Ali, K., "Component-Based Plug-and-Play Methodologies for Embedded Technology Development," *AIAA Infotech Conference,* Arlington, Virginia, 26-29 Sep 2005.